2023 IEEE International Conference on Robotics and Automation (ICRA 2023)
May 29 - June 2, 2023. London, UK

Experimental Workflow Implementation for Automatic Detection of Filament Deviation in 3D Robotic Printing Process

Xinrui Yang, Othman Lakhal, Abdelkader Belarouci, Kamal Youcef-Toumi and Rochdi Merzouki

Abstract— **Robotic 3D Concrete Printing (3DCP) is a process of additive manufacturing using building materials. The system that performs 3DCP is a complex system consisting of multiple parts that are independent of each other. However, conventional 3DCP workflows usually lack automatic monitoring of print quality which can be easily affected for various reasons. This paper proposes an integrated workflow of automatic detection of filament deviation in a 3DCP process. The deformation of the filament is adopted as the criterion for print quality evaluation. A Deep Learning-morphology-based filament width estimation method is developed, and a filament deviation detection algorithm with presence of parametric uncertainties is proposed. This workflow allows to detect width deviations in the printed filament by considering several parameters of the printing system. The integrated workflow is implemented and tested through on-site printing tests.**

I. Introduction

3D-Concrete Printing (3DCP) is a form of Additive Manufacturing (AM) using cementitious materials specifically for the fabrication of construction components or urban furniture [1]. 3DCP is an uprising topic that has attracted the attention of the research field and is widely used in the construction industry, thanks to its benefits including labor savings, and reduced construction time, while increasing the complexity of the building.

There exist two different printing strategies: injection and deposition/extrusion-based printing. In this paper, we focus on the more widely used extrusion-based printing. As a multidisciplinary field, 3DCP involves materials science, automation, robotics, etc., and the print quality is affected by different factors, including material mixing proportion, environmental conditions and printing system parameters, thus, the cooperation between different parts of 3DCP remains a challenge. In daily practical printing scenarios, it is possible that the material properties will be different for each print job, as different source and different mixing proportion of materials can significantly affect the rheological and viscosity properties of the concrete mixture, thus changing its fluid behavior during deposition, which can further affect the quality of printed structures [2]. The operating parameters of the printing system can also affect the characteristics of the material and thus the print quality [3]. There are two main controllable parameters in the printing system: nozzle movement speed and material flow rate, which can be controlled by changing the speed of the guiding robot and command of pumping voltage, respectively. The influence of printing parameters on the material distribution of spay-based concrete printing filament is studied in [4], and an analytical model is developed that helps choosing printing parameters according to the filament size. However, when the print job is performed in uncontrolled environment with perturbations (e.g. outdoors), the parameters determined in a controlled environment will not match the material state sufficiently to maintain print quality because the behavior of the material changes during the printing process due to environmental changes and internal chemical reactions, as it is in transient status.

One of the main challenges for many experiments is to select the ideal parameters for the printing system and to update them adaptively according to the print quality. In [5], trial-and-error tests were carried out inside a controlled environment for determining the nozzle speed and pump voltage, these parameters are to be kept constant during the printing phase and should be updated manually by an operator if the width of the printed filament deviates. Research works have also shown that two printing parameters (i.e. nozzle travel speed and material volumetric flow rate) can significantly affect the size of the printed filament [6]. As for the evaluation of print quality, the deformation of printed filament has been used as a criterion for real-time or post-printing quality assessment in several research works [7], [8].

Conventional 3DCP workflow requires an inspector to monitor the print quality and intervene in printing parameters when filament size deviates during printing. To address this limitation, an automatic filament deformation detection method is needed to automate the printing process. In the literature, Computer Vision (CV) based methods have been adopted for filament deformation based print quality assessment. In [9], [10], edge detection method is adopted for measurement of the width of printing filament. However, conventional CV algorithms are subject to lighting conditions and backgrounds, such as print beds or filaments stacked on top of each other, while Deep Learning (DL) can achiever higher accuracy in semantic or instance segmentation tasks [11]. Deep learning methods have been used in [12] for quality inspection of printed concrete objects in the post-printing stage, a deep convolutional neural network (DCNN) has been trained to segment the entire printed structure,

X. Yang, O. Lakhal, A. Belarouci and R. Merzouki are with University of Lille, CRIStAL, CNRS-UMR 9189, Avenue Paul Langevin, 59655 Villeneuve d'Ascq, France, email: xinrui.yang@univ-lille.fr. K. Youcef-Toumi is with Department of Mechanical Engineering at Massachusetts Institute of Technology 02139, Cambridge, MA, USA.

979-8-3503-2365-8/23/$31.00 ©2023 IEEE

followed by a CV line detection algorithm for layer height deformation detection. In [13], DCNN has been used for defects and deformation detection of filament height using side view filament images. However, few use DL methods for inline print quality inspection tasks by considering filament width rather than height.

In this paper, an integrated workflow of robotic 3DCP is proposed, focusing on the detection of deviations in printed filaments. A print quality monitoring process is integrated into the conventional 3DCP workflow, this process includes a vision system that automatically detects deviations in filament width with parametric uncertainties. The filament width deviation detection is realized by two steps: firstly, a filament width estimation algorithm based on Deep Learning and morphology is developed to estimate the width of printed filaments in real time. Secondly, residual signal and adaptive threshold are generated to detect filament width deviation. The residual signal is derived from geometric relationships that reflect the deposition state of the material, and adaptive thresholds with consideration of parametric uncertainty helps to detect deviation and avoid false alarm in the monitoring of the printing process. The output of the quality monitoring part helps to determine the operation status of the printing process. If filament width deviation is detected, the printing system can be reconfigured to compensate by adjusting the nozzle movement speed [14] or the pumping speed. By considering multiple parameters, this workflow improves the detection of printed filament deformation and contributes to future development of compensation strategy.

II. Workflow for Automatic Detection of Filament Deviation

In general, traditional workflows of robotic 3DCP processes are similar. In this section, the proposed integrated workflow is presented, the pre-processing of printing task and the printing system used throughout this work are reported, followed by the DL based filament deviation detection process.

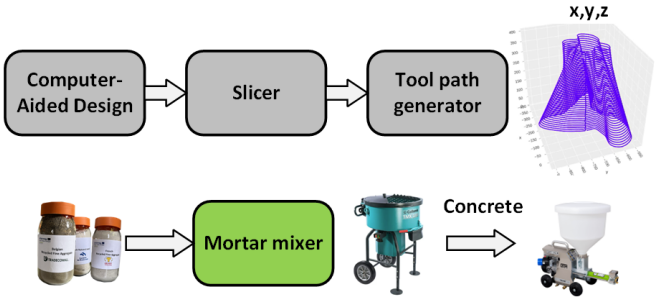

Fig. 1: Pre-processing of robotic 3DCP

A. Pre-processing of 3DCP

The pre-processing step of 3DCP concerns two parts: tool path generation for printer nozzle and material preparation. Fig.1 presents the pre-processing step.

1) Tool path generation: Firstly, a 3D geometry is designed with the help of Computer Aided Design (CAD) software (Rhino, Onshape, etc.). On the basis of the outer surface of the designed CAD geometry, slicing software (SlicerXL, Grasshopper 3D, etc.) will define the tool path that the 3D printer nozzle follows during the printing process. This step usually generates a file that contains a sequence of points along the tool path expressed by X, Y and Z coordinate. The file can be further translated in the programming language that is acceptable by the used robot. As 3DCP involves an additive mode of material deposit, the distance between two layers can affect the buildability of the filament. Usually, the design distance between the two layers should be less than the diameter of the nozzle to ensure buildable filament.

2) Material preparation: Secondly, the material is prepared according to a certain concrete batching inside a mortar mixer. The concrete batching (i.e. the mixing proportion of materials) is significantly important for 3DCP, because the rheological properties of the mixture should meet the requirement of printable materials. When the tool path is defined and the material is prepared, the printing system will be launched and calibrated to start printing, the materials will be deposited layer by layer to realize the designed geometry.

B. Printing system

The system that performs 3DCP process is a complex system composed by several component systems, as shown in Fig.2.

1) Robot: The robot used in this work is a Universal Robots UR10e 6-axis collaborative industrial manipulator robot. The robot is mounted on a platform that is fixed on the ground and a printer head is mounted on the end effector of the robot. The printer head is composed of a nozzle for the extrusion of materials, a flow rate sensor and two cameras. The nozzle has a circular outlet with a diameter of 20 mm, and a flow sensor is mounted at the nozzle's inlet to measure the flow of material as close as possible to the tip of the nozzle. During the printing process, the robot executes the tool path provided by the slicing step to guide the nozzle.

2) Pump and hose: An MAI 2PUMP-PICTOR mortar pump is used for the generation of material flow. A pressure sensor is installed at the outlet of the pump for the monitoring of pumping pressure. The pump and the printer nozzle on the robot are joined via a mortar hose, with length of 10 m and diameter of 40 mm.

3) Available sensors: Multiple sensors are available for obtaining redundant information and measurements in real-time:

- A flow rate meter is installed between the outlet of the hose and the nozzle to measure the flow rate of the material at the printer nozzle.
- Two Basler industrial Gigabit Ethernet (GigE) cameras are fixed on both sides of the printer head. The two cameras are mounted on the same horizontal line with their optical axes perpendicular to the printing bed. The distance between the cameras and the tip of the nozzle is fixed to 480 mm. The cameras allow to obtain

top-view images with 492 x 658 pixels, they are used for the measurement of the width of freshly printed filament and the detection of width deviation. The two cameras work alternately, according to the direction of movement of the nozzle, so that the captured image always contains the freshly printed filament and not the filament of the previous layer.

- The position and speed of the Tool Center Point (TCP) of the robot is provided by its built-in sensors.

The control command of the robot and the pump, as well as the data communication among all sensors is realized through Robot Operating System (ROS) framework running on a DELL workstation.

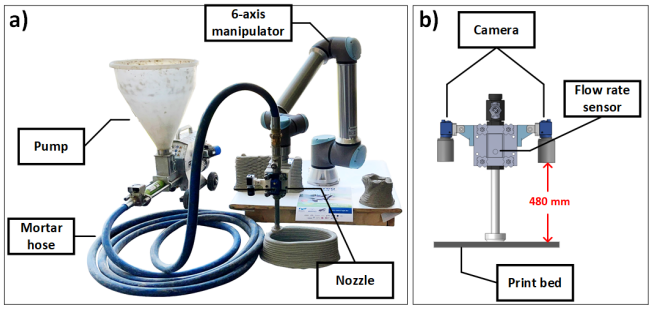

Fig. 2: 3D Concrete Printing System. a) Overall view of printing system. b) Nozzle equipped with multiple sensors.

C. Vision based estimation of filament width

This part presents briefly a qualitative approach for the real-time estimation of filament width, a more detailed description of this approach is reported in [14]. The estimation approach is data-driven and has adopted a DL instance segmentation model for the identification of freshly printed filament from an image taken by the visual sensors on the printer head. The morphological medial axis transform is then used for extracting a center line of the identified filament segment and calculating the overall width of the filament segment in image frame. Then a frame transformation step is applied to transform the unit of width from pixels to millimeters. The estimated value of filament width is used for the detection of filament deviation.

1) Segmentation of Filament: This part is realized by exploring the top-view images of freshly printed filaments provided by the cameras that are mentioned in Section II-B.3. We adopted a DL instance segmentation model, namely Mask RCNN [15], to segment the filament in real-time. Mask RCNN has been implemented in other single-target-single-class instance segmentation tasks in multiple fields including medical imaging, agriculture [16] and civil engineering [17], but has not been applied yet in the monitoring and control of 3DCP process. It has shown better performance compared to other models in term of efficiency and precision. An image dataset is collected and annotated throughout many printing sessions. The model is trained upon the dataset and reached 88.8% average precision at 0.5 IoU and 79.8% average precision at 0.75 IoU on a validation dataset.

Fig.3a shows an example of filament segmentation result of the model, the model generates a binary mask that covers the filament area in the input image. In the real-time implementation, we choose a smaller RoI (Region of Interest), so that the image contains a shorter segment of filament, which helps to improve the precision of width calculation.

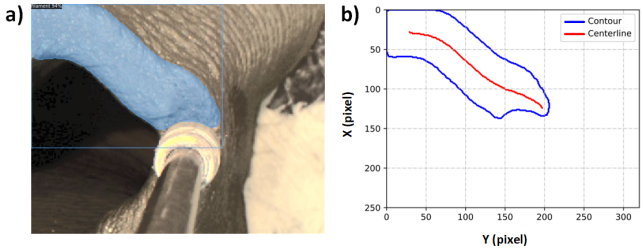

Fig. 3: a) Output of Mask RCNN. b) Contour and center line of filament reconstructed in image frame.

2) Filament width estimation: A morphology-based filament width estimation approach is developed. Based on the binary mask provided by the instance segmentation model, we can estimate the overall width of the freshly printed filament segment in mm. Fig.3b shows the filament contour and center line extracted by this step.

In the implementation of the filament segmentation model, the sampling rate guarantees that no filament segments will be missed by the cameras. During the printing process, the camera captures an image every 0.1 s. The speed of the nozzle is limited within a suitable range of 3 cm/s $\sim$ 15 cm/s for 3DCP, hence the nozzle can only move a maximum of 1.5 cm between two sample images taken by the cameras. Therefore, we have a continuous record of material depositing during the process.

Since we apply a smaller RoI, a filament segment with the length of around 5 cm $\sim$ 10 cm is considered in each estimation. The estimation of the overall width of a filament segment can be realized by two steps: center line extraction and image frame transformation. Firstly, we apply the morphological medial axis transform method to the binary mask of the filament to find the center line of the segmented filament and obtain the local width of the filament in pixels at each point of the center line. The overall width (in image frame) of the considered filament segment is then represented by the statistic mode (i.e. the peak of its histogram) of local width values. Secondly, we apply frame transformation in order to transform the unit of the estimated width from pixels to millimeters. By calculating the difference between the desired filament width w^d and the estimated width $\hat{w}$, we obtain the estimated error of filament width $\hat{e_w}$:

$$\hat{e_w} = w^d - \hat{w} \tag{1}$$

The desired filament width is determined by the design and slicing step. The estimated width $\hat{w}$ and error of width $\hat{e_w}$ are used in the following step of filament deviation detection.

D. Automatic detection of filament deviation

The approach for the detection of filament deviation is presented in this section. The approach is based on a geometric model, a residual signal is generated with presence of parametric uncertainties, and adaptive thresholds are generated for the detection of filament deviation [18]. In an ideal printing scenario, the width of the deposited filament conforms the desired value given by the pre-processing step, resulting in filaments with uniform width. However, in real continuous printing case, two scenarios could happen in term of filament deformation: 1) increased filament width, due to over-extrusion of materials; 2) reduced filament width, due to under-extrusion of materials, either case will result in a deviation of filament width. In order to solve this problem, a deviation detection algorithm is necessary.

A description of parameters that are considered in this study is given in Table I. In practical printing tasks, the nozzle speed is usually limited within 3 cm/s $\sim$ 15 cm/s to avoid collapse due to material property, consequently, throughout the study, we adopt the assumption that the robot operates in low speed and acceleration in permanent continuous printing mode. Let us consider a classic geometric

TABLE I: Description of parameters

Variable	Description	Unit
Q	Volumetric flow rate	ml/s
w	Filament width	cm
h	Filament height	cm
v	Nozzle speed	cm/s

model of nozzle-filament describing the material deposition during printing process [19]. In an ideal printing scenario, we consider that the freshly deposited filament is in the shape of a rectangular cuboid, with uniform height and width, as shown in Fig.4. According to the model, the following

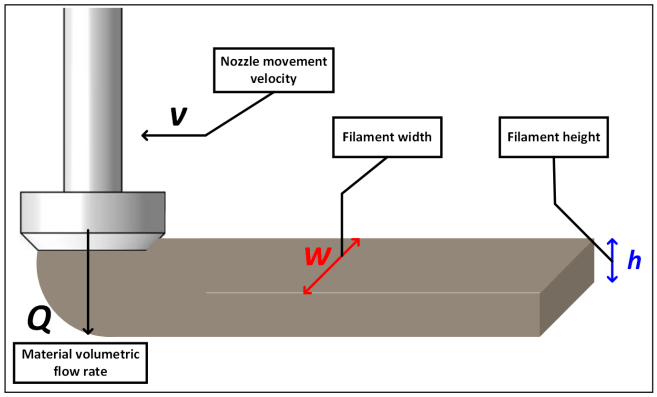

Fig. 4: Geometric model of nozzle-filament during a printing process

relation can be established:

$$Q = whv \tag{2}$$

However, in real printing scenarios, the uncertainties in the measurement of filament width and height are considered:

$$\begin{aligned} w &= w_n(1+\delta_w) \\ h &= h_n(1+\delta_h) \end{aligned} \tag{3}$$

therefore,

$$Q = w_n(1+\delta_w)h_n(1+\delta_h)v \tag{4}$$

where w_n and h_n denote the nominal values of filament width and height, respectively, and δ_w and δ_h represent the multiplicative uncertainties of filament width and height. In this study, the nominal value of height h_n is considered to be equal to the layer height (9 mm) defined in the tool path generation step, which is relatively small compared to the width. The nominal value of width w_n is identified through a statistical approach. During an observation window, its nominal value is described by its mean value:

$$w_n = \frac{1}{k}\sum_{i=1}^{k} w_i \tag{5}$$

with the multiplicative uncertainty

$$\delta_w = \frac{\Delta_w}{w_n} \tag{6}$$

The additive uncertainty of filament width Δ_w is given by the difference between the maximum value and the nominal value. The multiplicative uncertainty of filament height δ_h is determined by manual measurements of printed shapes and a fixed value of 10% is considered. Therefore, the following analytical relation cab be derived:

$$Q - w_n h_n v - (w_n h_n \delta_h v + w_n \delta_w h_n v + w_n h_n v \delta_h \delta_w) = 0 \tag{7}$$

The equation 7 consists of two parts: 1) a nominal part r called residual for describing the model and 2) the uncertain part a which is used for the generation of adaptive thresholds during normal operation of the system, as shown below:

$$\begin{cases} r = Q - w_n h_n v \\ a = |w_n h_n \delta_h v| + |w_n \delta_w h_n v| + |w_n h_n v \delta_h \delta_w| \end{cases} \tag{8}$$

In equation 8, a represents the upper threshold and the lower threshold can be given by $-a$, forming an envelope of the residual signal, such that in normal printing operation:

$$-a \leq r \leq a \tag{9}$$

By tracking the residual signals r in real-time, we are able to monitor the print quality and to detect deviation when it occurs.

E. Integrated workflow

The proposed workflow of filament deviation detection during a printing process combines the steps depicted above and integrate them into a traditional 3DCP workflow. The workflow, as shown in Fig.5, monitors the quality of filament in term of width and detects filament deviation. Once the printing task is launched, the system operates in continuous printing mode with fixed speed. The digital and image data collected by sensors embedded in the system are sent to the automatic deviation detection system, including v, Q and top view filament images. The detection system firstly

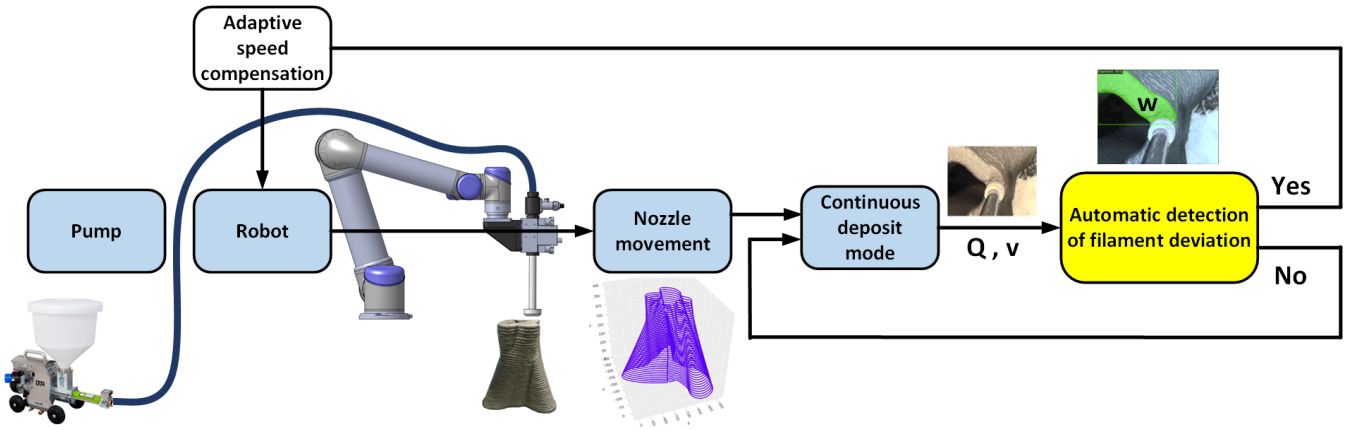

Fig. 5: The integrated workflow of automatic filament deviation detection in a 3DCP process.

estimates the overall width of freshly printed filament, and then generates residual signal and adaptive threshold using the received data. The residual signal r in Equation 8 is dedicated to the detection of filament deviation. Once the residual signal exceeds the adaptive threshold, deviation alarm will be sent to the control system of the robot, then a decision should be made in order to compensate to this deviation. Under cases of over-extrusion or under-extrusion, there are two options of intervention in order to maintain the residual inside the threshold envelope: updating the pumping flow by controlling the pump voltage command, or updating the nozzle speed. Since there exists a latency in the change of pumping flow when the voltage command is updated, updating the speed of the robot would be a faster and more accurate solution.

Considering the dynamic of a nozzle guided by a manipulator, operating in conditions of low speed and acceleration in continuous printing mode with speed v. It concerns a nozzle system with mass m, with viscous friction f, the following control law is developed in [14]:

$$U = m.\dot{v^d} + f.v^d + K_p.\varepsilon + K_d.\dot{\varepsilon} + (\frac{Q}{wh} - v).sign(r) \quad (10)$$

where K_p and K_d are the proportional and derivative parameters of the PD nozzle speed controller, r is the residual signal given in equation 8, $\varepsilon = v^d - v$ is the speed error and the *signum* function is adopted as a switch between increasing and reducing the speed.

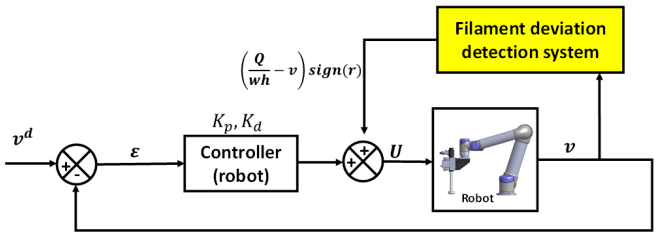

Fig. 6: Block diagram for the speed compensation

III. Experimental results

Printing experiments were carried out to implement the integrated workflow of filament deviation detection in the printing process.

A. Printing conditions

The material that was used throughout the experiments conforms several characteristics. The concrete batching as shown in Tab.II is respected. This mixture of material has a density of 2.25 g/cm^3 and does not have stable viscosity due to its nature of non-Newtonian fluid. A Collomix TMX 1000 mortar mixer is used for preparing the concrete batching. The printing tasks were performed in stable indoor environment with temperature of approximately 26°C. The distance between two layers of the tool path is fixed to 0.9 mm, which is much less than the nozzle diameter 20mm, to ensure buildable filaments. The upper bound of nozzle speed limit is set to 10 cm/s. A rectangular-shaped object

TABLE II: Batching of concrete mixing

Cement	35 kg
Recycled Sand	38.5 kg
Water	12.1 kg
Superplasticizer	875 g
Viscosity modifying agent (VMA)	70 g

is designed for printing experiment. The nozzle follows the same path at each layer, which is a rectangle of 30 cm x 60 cm. During the printing procedure, the integrated deviation detection system is able to collect data while estimating the filament width. The residual signal is generated in real time for the detection of deviation. The processing time from each top-view image to the generation of residual is around 0.3 s.

B. Results and discussion

In practical printing tests, 3 scenarios can be observed, as shown in Fig.7. In the case of normal operation of the printing system, the deposited filament has an overall uniform width that varies slightly around the desired value,

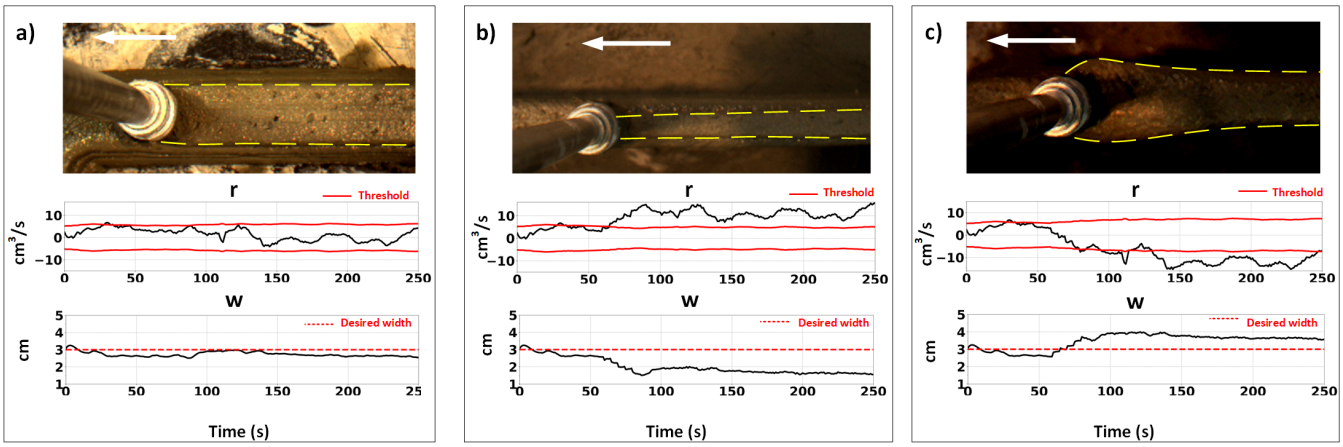

Fig. 7: 3 scenarios of filament deviation, the white arrow represents the direction of nozzle movement. a) Normal operation mode, with uniform filament width. b) Under-extrusion, filament width less than desired value with positive residual. c) Over-extrusion, filament width greater than desired value with negative residual.

the residual stays inside the threshold envelop, the continuous printing mode can be maintained. In Fig.7b, the filament width reduces, which matches a case of under-extrusion. In this case a positive residual is obtained. In another case in Fig.7c, where the filament width is increasing, a negative residual is obtained. When the residual exceeds the threshold and stables outside the threshold envelope, it is considered that a deviation occurs, and an intervention is to be applied in order that the nozzle speed matches the flow rate.

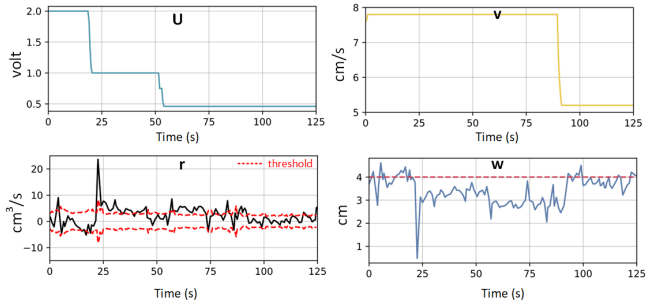

Fig. 8: Detection of filament deviation and compensation by updating speed. U: pump voltage, v: nozzle speed, r: residual signal, w: filament width.

As shown in Fig.8, filament deviation can be provoked by modifying the pump command voltage, as an imperfect combination of nozzle speed and pumping flow usually results in abnormality in material deposition. When the pumping flow is reduced, the filament width deviates from the stable value and the residual indicates that a deviation occurs. For observation purposes, the deviation was held for a period of time until the speed adjustment was applied. Despite the fact that speed adjustment is able to compensate for deviations, in some cases it is necessary to regulate the pumping flow as well (e.g. when the nozzle speed has reached its limit). In addition to detection, future works will study the isolation of filament deviation. Indeed, compensation by adjusting the two coupled parameters (nozzle speed and pumping voltage) can break some limits and can deal with more complex cases of deformations.

IV. CONCLUSIONS

In this paper, an integrated workflow of filament deviation detection in a 3DCP process is developed. The workflow combines a vision-based filament deviation detection system with a conventional 3DCP system. The deviation detection approach consists of two steps: firstly, a filament width estimation step based on Deep Learning and morphology medial axis transform is developed; secondly, a deviation detection step with presence of parametric uncertainties is considered to detect filament deviation automatically. The integrated workflow improves the robotic 3DCP process by providing solution to online print quality monitoring. The workflow has been implemented experimentally, the results shows its ability in detecting filament deviation and improving the print quality. When deviation occurs, a compensation step will be applied by updating the nozzle speed, future works will be carried out to improve the reconfiguration of printing parameters during robotic 3DCP process.

ACKNOWLEDGMENT

This work has been realized with the support of EU funding through Interreg project CIRMAP NWE 1062.

REFERENCES

[1] J. Xiao, G. Ji, Y. Zhang, G. Ma, V. Mechtcherine, J. Pan, L. Wang, T. Ding, Z. Duan, and S. Du, "Large-scale 3d printing concrete technology: Current status and future opportunities," *Cement and Concrete Composites*, vol. 122, p. 104115, 2021.

[2] R. A. Buswell, W. L. De Silva, S. Z. Jones, and J. Dirrenberger, "3d printing using concrete extrusion: A roadmap for research," *Cement and Concrete Research*, vol. 112, pp. 37–49, 2018.

[3] H. Zhang, J. Wang, Y. Liu, X. Zhang, and Z. Zhao, "Effect of processing parameters on the printing quality of 3d printed composite cement-based materials," *Materials Letters*, vol. 308, p. 131271, 2022.

[4] B. Lu, M. Li, T. N. Wong, and S. Qian, "Effect of printing parameters on material distribution in spray-based 3d concrete printing (s-3dcp)," *Automation in Construction*, vol. 124, p. 103570, 2021.

[5] O. Lakhal, T. Chettibi, A. Belarouci, G. Dherbomez, and R. Merzouki, "Robotized additive manufacturing of funicular architectural geometries based on building materials," *IEEE/ASME Transactions on Mechatronics*, vol. 25, no. 5, pp. 2387–2397, 2020.
[6] Y. W. D. Tay, M. Y. Li, and M. J. Tan, "Effect of printing parameters in 3d concrete printing: Printing region and support structures," *Journal of Materials Processing Technology*, vol. 271, pp. 261–270, 2019.
[7] J. Reinold, V. N. Nerella, V. Mechtcherine, and G. Meschke, "Extrusion process simulation and layer shape prediction during 3d-concrete-printing using the particle finite element method," *Automation in Construction*, vol. 136, p. 104173, 2022.
[8] F. Bos, R. Wolfs, Z. Ahmed, and T. Salet, "Additive manufacturing of concrete in construction: potentials and challenges of 3d concrete printing," *Virtual and physical prototyping*, vol. 11, no. 3, pp. 209–225, 2016.
[9] A. Kazemian, X. Yuan, O. Davtalab, and B. Khoshnevis, "Computer vision for real-time extrusion quality monitoring and control in robotic construction," *Automation in Construction*, vol. 101, pp. 92–98, 2019.
[10] E. S. Barjuei, E. Courteille, D. Rangeard, F. Marie, and A. Perrot, "Real-time vision-based control of industrial manipulators for layer-width setting in concrete 3d printing applications," *Advances in Industrial and Manufacturing Engineering*, p. 100094, 2022.
[11] N. O'Mahony, S. Campbell, A. Carvalho, S. Harapanahalli, G. V. Hernandez, L. Krpalkova, D. Riordan, and J. Walsh, "Deep learning vs. traditional computer vision," in *Science and information conference*. Springer, 2019, pp. 128–144.
[12] O. Davtalab, A. Kazemian, X. Yuan, and B. Khoshnevis, "Automated inspection in robotic additive manufacturing using deep learning for layer deformation detection," *Journal of Intelligent Manufacturing*, pp. 1–14, 2020.
[13] R. Rill-García, E. Dokladalova, P. Dokládal, J.-F. Caron, R. Mesnil, P. Margerit, and M. Charrier, "Inline monitoring of 3d concrete printing using computer vision," *Additive Manufacturing*, vol. 60, p. 103175, 2022.
[14] X. Yang, O. Lakhal, A. Belarouci, and R. Merzouki, "Adaptive deposit compensation of construction materials in a 3d printing process," in *2022 IEEE/ASME International Conference on Advanced Intelligent Mechatronics (AIM)*. IEEE, 2022, pp. 658–663.
[15] K. He, G. Gkioxari, P. Dollár, and R. Girshick, "Mask r-cnn," in *Proceedings of the IEEE international conference on computer vision*, 2017, pp. 2961–2969.
[16] K. Hameed, D. Chai, and A. Rassau, "Score-based mask edge improvement of mask-rcnn for segmentation of fruit and vegetables," *Expert Systems with Applications*, vol. 190, p. 116205, 2022.
[17] M. Kahouadji, O. Lakhal, X. Yang, A. Belarouci, and R. Merzouki, "System of robotic systems for crack predictive maintenance," in *2021 16th International Conference of System of Systems Engineering (SoSE)*. IEEE, 2021, pp. 197–202.
[18] M. A. Djeziri, R. Merzouki, and B. O. Bouamama, "Robust monitoring of an electric vehicle with structured and unstructured uncertainties," *IEEE transactions on vehicular technology*, vol. 58, no. 9, pp. 4710–4719, 2009.
[19] A. Anton, L. Reiter, T. Wangler, V. Frangez, R. J. Flatt, and B. Dillenburger, "A 3d concrete printing prefabrication platform for bespoke columns," *Automation in Construction*, vol. 122, p. 103467, 2021.